Ind. J. Pharm. Edu. Res., 2027; 61(1):10.5530/ijper.20262572.
https://www.ijper.org

Original Article

Multi-Target Mechanisms of *Dipsacus inermis* Against Osteoporosis via Inhibition of Nitric Oxide and NF-κB/ COX-2 Pathway

Tingyu Min[1,#], Songjun Li[2,#], Xibin Zhang[3,*]

[1]Department of Orthopaedics, Huai'an No 4 People's Hospital, Huai'an Jiangsu, CHINA.
[2]Department of Orthopedics, The Fifth Affiliated Hospital of ZunYi Medical University, Zhuhai, ZhuHai Guangdong, CHINA.
[3]Department of Traumatic Orthopedics, Zhejiang Orthopedics Hospital, Hangzhou Zhejiang, CHINA.
[#]The Authors Contributed Equally to this Work.

ABSTRACT

Background: Osteoporosis is a severe bone disease that has few effective treatment options and major side effects. *Dipsacus inermis*, a conventional medicinal plant, demonstrates potential via multi-target regulation of inflammatory and bone remodeling pathways. **Aim:** To assess the anti-osteoporotic efficacy of *Dipsacus inermis* via a combination of computational and experimental approaches. **Materials and Methods:** Phytochemical analysis was conducted using the TCMID database. Target prediction using SuperPred, SwissTargetPrediction, and TCMID, subsequently including osteoporosis targets from Gene Cards. Protein–protein interaction networks were generated with STRING followed by analysis in Cytoscape, with hub analysis conducted by Cytohubba. Functional enrichment was conducted via Enrichr. Molecular docking investigations focused on *ESR1*, *NFKB1*, and *PTGS2*. Experimental tests included the Griess reaction, COX-2 ELISA, and MTT cytotoxicity assessment on J774A.1 cells. **Results:** Screening revealed 15 phytochemicals, further refined to five principal compounds: Ursolic Acid, Loganic Acid, Loganin, β-Sitosterol, and Chlorogenic Acid. Target predictions produced 110, 116, and 65 targets from SuperPred, Swiss Target Prediction, and TCMID, respectively, with 51 shared targets. By filtering osteoporosis targets from 7,231 to 1,038 using Gene Cards, the overlap yielded 30 common genes. The established PPI network exhibited 30 nodes, 89 edges, an average node degree of 5.93, and a clustering coefficient of 0.526 (p=1.11e-16). Docking findings indicated binding affinities of –8.567 kcal/mol for β-Sitosterol–*NFKB1* and –8.305 kcal/mol for Ursolic Acid–*PTGS2*/COX-2. Experimental results indicated that treatment decreased nitric oxide levels from 20 µM to 9 µM and COX-2 expression from 625 pg/mL to 315 pg/mL at a concentration of 400 µg/mL; cell viability declined to 45% at 800 µg/mL. Additionally. Significant inhibition by *Dipsacus inermis* on LPS-induced NF-κB activation was observed in J774A.1 macrophages following concentration-dependent pattern. **Conclusion:** *Dipsacus inermis* has considerable multi-target efficacy against osteoporosis and inflammatory pathways, underscoring its potential as a new therapeutic agent.

Keywords: *Dipsacus inermis*, Inflammatory Pathways, Molecular Docking, Network Pharmacology, Osteoporosis, Traditional Chinese Medicine.

Correspondence:
Dr. Xibin Zhang
Department of Traumatic Orthopedics, Zhejiang Orthopedics Hospital, Hangzhou Zhejiang-310000, CHINA.
Email: zhangxibin999@outlook.com
ORCID: 0009-0003-7200-6436

Received: 18-03-2026;
Revised: 08-05-2026;
Accepted: 24-07-2026.

INTRODUCTION

Osteoporosis is a systemic skeletal condition defined by reduced bone mass and microarchitectural deterioration that leads to bone fragility and an increased risk of fractures.[1] Globally, osteoporosis has reached epidemic proportions, particularly in aging populations, and is associated with significant morbidity and lethality. Millions of fractures occur annually due to the disorder, with hip fractures being particularly lethal due to high complications and mortality rates.[2] Despite the development of various pharmacological treatments-including bisphosphonates, selective estrogen receptor modulators, and parathyroid hormone analogs-current therapies present several shortcomings.[3] Many treatments exhibit limited efficacy in reversing bone loss, are often associated with adverse side effects, and suffer from issues related to patient adherence.[4] These challenges underscore the need for alternative therapeutic approaches with enhanced safety and improved clinical outcomes.

More recently, network-pharmacology has developed as promising strategy in both Traditional Chinese Medicine

DOI: 10.5530/ijper.20262572

Copyright Information :
Copyright Author (s) 2027 Distributed under Creative Commons CC-BY 4.0

Publishing Partner : Manuscript Technomedia. [www.mstechnomedia.com]

(TCM) and modern drug discovery.[5] Unlike the "one-drug, one-target" paradigm, network pharmacology embraces a holistic view where multiple bioactive compounds interact synergistically with various targets. This systems-level approach is especially relevant for complex diseases like osteoporosis, where a multifaceted pathology may benefit from targeting multiple molecular pathways simultaneously. TCM has a long history of utilizing herbal formulations that inherently involve a blend of compounds, supporting the rationality of exploring network-based interactions.[6] Integrating network pharmacology with TCM not only aids in elucidating the mechanisms underlying the therapeutic actions of ancient herbal remedies but also contributes valuable insights into modern multi-target drug development.

A critical component of modern pharmacological research is molecular docking, a computational technique that predicts the binding orientation and interaction affinity among small molecules and proteins.[7] In drug discovery, molecular docking serves as a virtual screening tool that helps in identifying promising bioactive compounds by evaluating their potential to bind with high affinity to disease-relevant targets. The method combines principles from structural biology and medicinal chemistry, and its application has significantly accelerated the early stages of drug design. By simulating ligand-target interactions *in silico*, researchers can prioritize compounds for experimental validation, thereby reducing both time and cost in the drug development pipeline.

Dipsacus inermis, a medicinal herb used in Traditional Chinese medicine, has recently attracted attention owing to its reported pharmacological and phytochemical attributes.[8] Historically, *Dipsacus* species have been prescribed for various ailments including musculoskeletal disorders, inflammation, and bone healing.[9] Research on the phytochemistry of *Dipsacus inermis* has uncovered components such as triterpenoids, iridoids, and sterols that exhibit diverse biological activities.[10] Despite its traditional usage, molecular mechanisms underlying *Dipsacus inermis* to bone health remain inadequately characterized. Recent advances in network pharmacology and molecular docking provide an ideal framework to explore the potential role of this herb against osteoporosis.

The rationale behind this study is to systematically investigate *Dipsacus inermis* by employing a combination of network pharmacology and molecular docking techniques. First, the complex phytochemical composition of the plant is analyzed to identify bioactive compounds that meet specific drug-like criteria. Next, a comprehensive target prediction is performed using multiple databases, and the overlap between predicted targets of *Dipsacus* compounds and molecular targets implicated in osteoporosis is determined. Finally, the most promising targets are further validated using molecular docking to assess the binding efficiency of selected phytochemicals. This integrative approach offers an innovative pathway to uncover multi-targeted therapeutic mechanisms, which could eventually translate into novel strategies for prevention and overcoming of osteoporosis.

MATERIALS AND METHODS

Phytochemical Screening and Data Retrieval

Phytochemical screening of *Dipsacus inermis* was conducted using data extracted from the Traditional Chinese Medicine Integrated Database (TCMID).[11] TCMID 2.0 ("http://www.megabionet.org/tcmid/") is a comprehensive online repository that provides detailed information on herbal ingredients, associated compounds, and their targets within the context of traditional Chinese medicine. For this study, compounds were filtered based on two key criteria: a molecular weight between 200 and 500 Daltons to ensure adequate bioavailability (≥ 0.30) and suitability for drug-like (≥0.18) properties, and compliance with Lipinski's rule of five, which predicts the oral bioavailability of chemical compounds.[12] The use of TCMID allowed us to obtain a curated list of phytochemicals, streamlining the initial screening process and ensuring that only compounds with favorable pharmacokinetic properties were advanced for further analysis.

Target Prediction for Phytochemicals

To predict potential targets for the selected phytochemicals, three distinct and complementary databases were employed: SwissTargetPrediction ("https://swisstargetprediction.ch/"), SuperPred 3.0 ("https://prediction.charite.de/index.php"), and TCMID.[11,13,14] SwissTargetPrediction is an established web tool that utilizes both two-dimensional and three-dimensional similarity comparisons to predict the most likely macromolecular targets for bioactive small molecules. Its predictions are based on accumulated experimental bioactivity data, providing a significant framework for target identification. SuperPred functions in a similar capacity and offers target predictions by analyzing chemical similarities against a large reference dataset. Its algorithm not only identifies potential targets but also provides insights into binding affinities. The previously mentioned TCMID was also leveraged to cross-reference targets specifically related to TCM compounds.

Following target prediction, the outputs from all three databases were combined. Redundant targets were eliminated, and only those targets that appeared in at least two of the databases were retained. This filtering process was facilitated by the online tool JVenn ("https://jvenn.toulouse.inrae.fr/app/index.html"), which provides an interactive Venn diagram interface to visualize overlapping sets of data and to identify common target genes across multiple data sources.

Disease Target Identification

For the disease context, osteoporosis-related targets were extracted from the GeneCards database.[15] GeneCards ("https://

IN PRESS

www.genecards.org/") is a comprehensive gene-centric platform that integrates annotated and predicted data from a wide variety of genomic sources. In this study, gene selection was refined by adopting a stringent threshold-only genes with a GIFTS (gene inference and functionality scoring) score of 60% or above were considered.[16] This criterion ensured that the selected targets were highly relevant to the pathophysiology of osteoporosis.

Protein-Protein Interaction Network Analysis

Intersecting targets for compounds-disease were identified using the JVenn tool, thereby yielding an intersecting set of targets for further analysis. These common target genes were then submitted to the STRING (Search Tool for the Retrieval of Interacting Genes/Proteins; "https://string-db.org/") database.[17] It is a highly curated platform that integrates both known and predicted PPIs, drawing from experiments, databases, and computational predictions. For this study, a high-confidence threshold with a confidence score of 0.700 was applied, and unconnected nodes were excluded to refine the interaction network. The resulting PPI network was transferred and imported into Cytoscape V 3.10.4, an open-source software platform designed for complex network visualization and analysis. Within Cytoscape, the Cutohubba plugin was employed to identify hub genes by calculating network centrality measures such as Degree, Maximal Clique Centrality (MCC), and Closeness scores.

Gene Ontology and Pathways Analysis

To elucidate biological relevance of intersecting targets, enrichment analyses for Gene Ontology (GO) and signaling pathways were performed using the Enrichr ("https://maayanlab.cloud/Enrichr/") database.[18] Developed by the Icahn School of Medicine at Mount Sinai, Enrichr is an intuitive online tool that offers comprehensive enrichment analysis for gene sets. The targets were analyzed for enrichment in three GO categories: Biological Processes (BP), Cellular Components (CC), and Molecular Functions (MF). Furthermore, pathway analyses were performed using several contemporary pathway databases: KEGG (2021), Reactome Pathways (2024), and WikiPathways (2024). Reactome is an expert-curated, peer-reviewed database focusing on detailed biological pathways, while WikiPathways is community-driven, emphasizing openness and rapid updates. The analysis was based on adjusted *p*-values to rank the significance of the enriched terms, with the top 10 pathways and their associated genes being subsequently scrutinized.

Molecular Docking Validation

The final phase of the study involved molecular docking to validate high-scoring hub targets and the selected phytochemicals. Three key protein targets-*ESR1, NFKB1*, and *PTGS2* (also known as COX2)-selected for docking research based on prominent positions in the PPI network. Their three-dimensional structures were retrieved from the RCSB Protein Data Bank (PDB), which is the premier repository for structural data of biological macromolecules. The respective PDB IDs used were 6vpf (*ESR1*), 1cx2 (*NFKB1*), and 1nfk (*PTGS2*).[19-21] Prior to docking, the structures were prepared using BIOVIA Discovery Studio (V. 2025), a sophisticated software suite that enables the removal of native ligands, water molecules, and extraneous chains to generate clean receptor models. The phytochemicals chosen for the docking study-Ursolic acid, Loganic acid, Loganin, Beta-sitosterol, and Chlorogenic acid-were obtained from the PubChem database. PubChem, a widely recognized repository that provides comprehensive information on the chemical structures and properties of small molecules. The compounds were downloaded in a two-dimensional conformer format (.sdf) for subsequent processing. Finally, the Dockthor V.2 ("https://dockthor.lncc.br/v2/") online platform was used to conduct the molecular docking simulations.[22] It is a modern web-based tool that carries out advanced docking studies, providing detailed insights concerning the ways in which ligands and target proteins interact and the affinities for binding.

Chemicals and Reagents

All reagents employed in this study were of analytical grade and sourced from reputable suppliers. Methanol (HPLC grade) and Dimethyl Sulfoxide (DMSO) were procured from Sigma-Aldrich (St. Louis, MO, USA), while the cell extraction buffer, ELISA kits for COX-2, and accompanying reagents, including the Griess reagent system for nitric oxide estimation, were acquired from Promega (Madison, WI, USA). Additionally, Fetal Bovine Serum (FBS), Dulbecco's Modified Eagle Medium (DMEM), and penicillin-streptomycin solution used for cell culture maintenance were purchased from Gibco (Thermo Fisher Scientific, Waltham, MA, USA). All other chemicals and solvents utilized in the assays were sourced from either Merck (Darmstadt, Germany) or Thermo Fisher Scientific, ensuring consistent quality across all experimental procedures.

Collection of *Dipsacus inermis* Plant Material and Methanolic Extraction

Plant material of *Dipsacus inermis* was collected from various locations within Shanxi Province, China, during the flowering season to ensure maximum phytochemical yield. The collected samples were authenticated by a local botanist and subsequently air-dried at room temperature. The dried plant material was then finely powdered prior to extraction. The 100 grams of the powdered material was subjected to Soxhlet extraction using methanol as the solvent for a continuous period of 4 hr. The resulting *Dipsacus inermis* Methanolic Extract (DIME) was concentrated under reduced pressure in a rotary evaporator, and the solvent was completely removed to yield a dry extract, which was stored at 4°C until further analysis.

IN PRESS

Cell Culture

The murine macrophage cell line, J774A.1, was obtained from the American Type Culture Collection (TIB-67 ™, ATCC, Manassas, VA, USA). Cells were maintained in DMEM supplemented with 10% FBS, 100 U/mL penicillin, and 100 µg/mL streptomycin, and incubated in a humidified atmosphere at 37°C with 5% CO_2. Culture conditions were monitored routinely to ensure optimal cell viability and morphology, and all experiments were conducted using cells in the exponential growth phase. Routine mycoplasma testing was performed to confirm the absence of contamination.

Estimation of Nitric Oxide by Griess Reaction

Nitric Oxide (NO) production was quantified using the Griess reaction, which is a colorimetric assay that measures nitrite levels, a stable NO metabolite. After appropriate treatment, cell culture supernatants were collected and mixed with the Griess reagent (Sigma-Aldrich, St. Louis, MO, USA) according to the manufacturer's instructions. The reaction mixture was incubated at room temperature for 15 min, allowing the development of a pink azo dye whose intensity directly correlates with nitrite concentration. Absorbance was measured at 540 nm using a microplate reader, and nitrite concentrations were extrapolated from a standard curve generated using sodium nitrite. This assay was performed in triplicate to ensure accuracy and reproducibility.

Evaluation of COX-2

In this study, macrophages treated with DIME were stimulated with Lipopolysaccharide (LPS, 1 µg/mL) for 24 hr to elicit an inflammatory response. Following stimulation, cells were lysed using the extraction buffer provided in the COX-2 ELISA kit (Promega, Madison, WI, USA), and lysates were clarified by centrifugation at 18,000 × g for 20 min at 4°C. The supernatant was then collected and analyzed for Cyclooxygenase-2 (COX-2) levels using a quantitative ELISA, adhering strictly to the manufacturer's protocol. The optical density of each sample was measured at 450 nm using a microplate spectrophotometer. All experiments were conducted in triplicate to confirm data repeatability and assure statistical significance.

Evaluation of NF-κB

The effect of *Dipsacus inermis* extract on NF-κB p65 activation in J774A.1 murine macrophages was evaluated using a Mouse NF-κB p65 ELISA Kit (Cat# E-EL-M0672, Elabscience®) following the manufacturer's protocol. Cells were seeded at a density of 1×10^6 cells/well in 6-well plates and pretreated with extract concentrations of 25, 50, 100, 200, and 400 µg/mL for 2 hr prior to stimulation with lipopolysaccharide (LPS, 100 ng/mL) for 24 hr. Following incubation, nuclear extracts were prepared using a nuclear extraction kit (Cat# ab221978; Abcam), and 100 µL of sample per well was loaded in duplicates. Absorbance at 450 nm was recorded using a microplate reader (BMG LABTECH, ELISA Microplate Reader), and NF-κB p65 concentrations were interpolated using a four-parameter logistic standard curve.

MTT Assay

The cytotoxic effects of the *Dipsacus inermis* extract on the J774A.1 macrophage cell line were evaluated using the MTT assay. Cells were seeded in 96-well plates and subsequently exposed to a range of extract concentrations (0, 25, 50, 100, 200, 400, and 800 µg/mL) for a predetermined incubation period. Post-treatment, 20 µL of MTT reagent (Sigma-Aldrich, St. Louis, MO, USA) was added to each well, and plates were incubated at 37°C for 4 hr to allow the formation of formazan crystals by viable cells. The formed crystals were then solubilized in 100 µL of DMSO, and the absorbance was recorded at 570 nm using a microplate reader. This assay was carried out in triplicate for each treatment concentration to ensure the reliability and consistency of the results.

Statistical Analysis

The experimental data was analysed using Origin Pro 2025, using its plugin Multiple Comparison by following two-way ANOVA and Tuckey test. The presentation was 3 independent experiments set as mean ±SD. The significance was set at p values of 0.05, 0.01 and 0.001. The gene ontology and Pathways data was visualised using adjusted p-values from the Enricher database and by default statistical analysis was employed.

RESULTS

Phytochemical Screening and Compound Selection

The initial exploration of the TCMID yielded in total 15 phytochemical compounds associated with *Dipsacus inermis*. Application of our stringent selection criteria-focusing on parameters such as molecular weight range (200–500 Da) and adherence to Lipinski's rule-led to a refined subset of only five compounds (Table 1). The final list comprised Ursolic Acid, Loganic Acid, Loganin, β-Sitosterol, and Chlorogenic Acid. This narrowing down not only ensured a focus on compounds with optimal drug-like properties but also provided a significant foundation for subsequent target prediction and network analyses.

Integrative Target Prediction Using Multi-Database Approach

The integrated target prediction approach combined outputs from three independent databases: SuperPred, SwissTargetPrediction, and TCMID. For the five selected phytochemicals and the plant itself, SuperPred predicted 110 targets, SwissTargetPrediction identified 116 targets, and TCMID contributed 65 targets (Figure 1A). A comparative analysis using an intersection strategy revealed that 51 targets were common between at least two of these databases (Suppl. Table S1). This intersection of targets

IN PRESS

increases the reliability of the predicted molecular interactions and provides a targeted list for further exploration in the context of osteoporosis treatment.

Identification of Disease-Specific Targets

The GeneCards database was employed to compile targets associated with osteoporosis. A comprehensive search yielded 7231 initial targets linked to the disease. To enhance target specificity, these were subsequently filtered by a stringent threshold, keeping only those with a GIFTS score of 60% or higher. This approach refined the list to 1038 osteoporosis-related targets (Suppl. Table S2), ensuring that only those with significant functional relevance and supporting evidence were carried forward in the analysis.

PPI Network Analysis

To elucidate potential interactions between the plant-derived targets and those related to osteoporosis, the 51 targets obtained

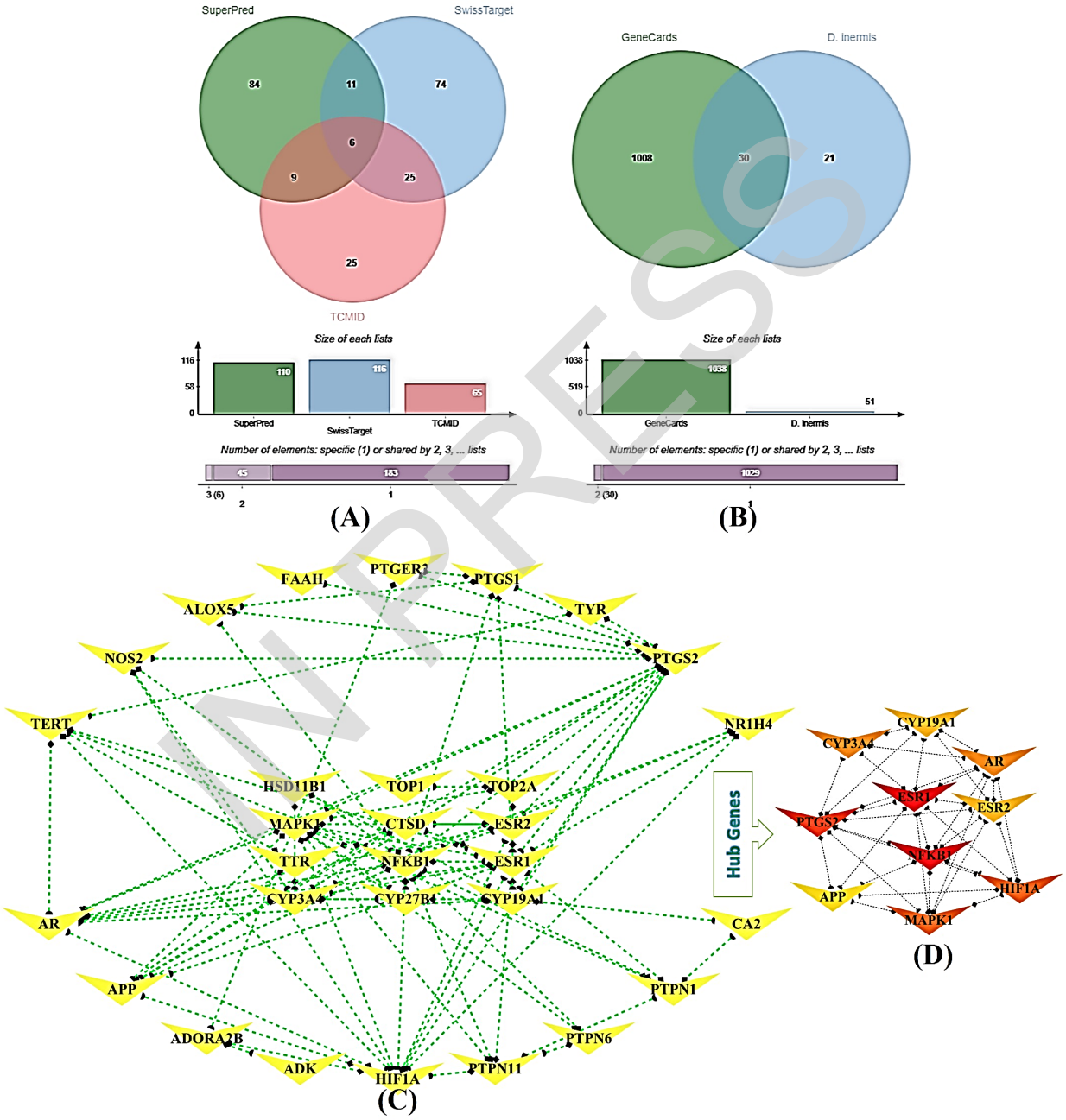
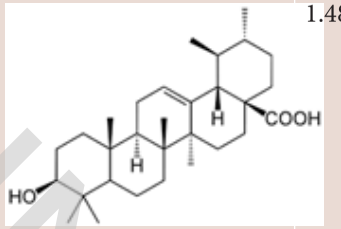
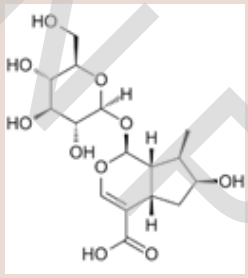
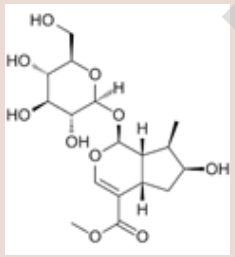
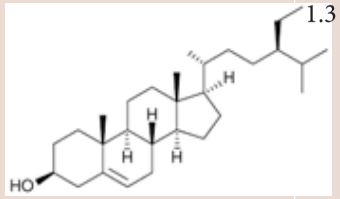
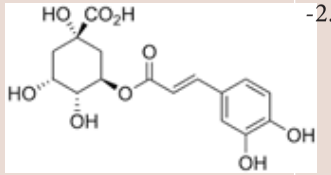


Figure 1: (A) Venn diagram illustrating the number of targets predicted by SuperPred (110 targets), SwissTargetPrediction (116 targets), and TCMID (65 targets) for the selected phytochemicals and Dipsacus inermis, emphasizing the overall predicted target landscape. (B) A Venn diagram or intersection plot showing the 30 common targets obtained from the intersection of the 51 plant-derived targets and the 1038 osteoporosis-related targets, suggesting a potential mechanistic link. (C) Network diagram generated in Cytoscape showing 30 nodes and 89 edges corresponding to the common targets. (D) The figure highlights the identified 10 hub genes (e.g., ESR1, NFKB1, PTGS2, MAPK1, etc.) as determined by the Cytohubba plugin using Degree, Maximal Clique Centrality (MCC), and Closeness metrics.

IN PRESS

Table 1: **Phytochemical screening from TCMID yielded 15 compounds, refined to five (Ursolic Acid, Loganic Acid, Loganin, β-Sitosterol, Chlorogenic Acid) based on drug-likeness criteria.**

Ingredient ID	Formulae	Name	MW	Structure	AlogP	ML ogP	XlogP	# HBA	# HBD	PSA	# Rotatable Bond	# Ring	# Heavy Atom
TCMC2216	$C_{30}H_{48}O_3$	Ursolic Acid	456.36		1.4838	4.43	8.954	3	2	57.53	10	5	33
TCMC2661	$C_{16}H_{24}O_{10}$	Loganic Acid	376.14		-3.1798	2.12	-1.413	10	6	166.14	11	3	26
TCMC2681	$C_{17}H_{26}O_{10}$	Loganin	390.15		-2.9288	2.23	-1.092	10	5	155.14	12	3	27
TCMC801	$C_{29}H_{50}O$	Beta-Sitosterol	414.39		1.3	4.54	11.595	1	1	20.23	13	4	30
TCMC897	$C_{16}H_{18}O_9$	Chlorogenic Acid	354.1		-2.1962	2.23	-0.447	7	6	164.75	11	2	25

IN PRESS

from the phytochemical prediction were cross-referenced with the 1038 disease-associated targets. The intersection of these datasets resulted in the identification of 30 common targets, suggesting a plausible mechanistic link between *Dipsacus inermis* and osteoporosis modulation (Figure 1B). These 30 genes were further analyzed making use of the STRING database, which resulted in a network with 89 edges and 30 nodes (Suppl. Figure S1). The network metrics indicated an average local clustering coefficient of 0.526, and node degree of 5.93, while the expected edges remained at only 32, with a highly significant p-value of 1.11e-16. Visualization of the network in Cytoscape (Figure 1C), coupled with analysis using the Cytohubba plugin based on Degree, Maximal Clique Centrality (MCC), and Closeness measures, identified 10 hub genes: *ESR1, NFKB1, PTGS2, MAPK1, HIF1A, AR, CYP3A4, ESR2, CYP19A1,* and *APP* (Figure 1D and Table 2). These hub genes represent key nodes that may mediate the anti-osteoporotic effects of the plant.

GO and Pathways Enrichment Analysis

The 30 common targets were subsequently subjected to enrichment analysis using the Enrichr database to reveal their functional roles and associated pathways. The GO enrichment analysis demonstrated significant overrepresentation across the three categories: BP, Cellular CC, and MF (Figure 2). Hub genes implicated in important processes including the control of biosynthesis and metabolism, especially nitric oxide and estradiol, have been identified using network pharmacology. Genes such as APP, *ESR1*, and *PTGS2*, for example, play a key role in processes including nitric oxide biosynthesis and the positive control of biosynthesis (GO:0045429). Additionally, *ESR1* is a key player in the molecular processes of transcriptional regulation (GO:0001223, GO:0034056) and steroid hormone signalling (GO:0030518), which are linked to bone metabolism (Suppl. Table S3).

In parallel, pathway analysis highlighted significant enrichment in several critical pathways, including those reported in KEGG (2021), Reactome (2024), and WikiPathways (2024) (Figure 3). All reported enrichments were based on adjusted *p*-values, underscoring the statistical rigor and biological relevance of the findings. These analyses not only confirm the multi-target mechanism underlying the therapeutic potential of *Dipsacus inermis* but also shed light on the molecular underpinnings of its effects in osteoporosis. A common interaction was shown by a network for plant-compounds-targets-pathways involving all KEGG, Reactome and WikiPathways in Figure 4.

Molecular Docking Validation

To verify hub interactions, molecular docking was used between the key phytochemicals and the top three hub targets identified in the PPI network: *ESR1, NFKB1*, and *PTGS2*. The docking analysis was conducted using a state-of-the-art online platform and the following table summarizes the docking parameters and outcomes for each ligand–target complex:

The docking results demonstrate significant binding affinities of the bioactive compounds with the targets, with interaction energies suggesting favorable binding conformations. For instance, Ursolic acid exhibited a binding-energy of –8.214 kcal/mol with *ESR1* and

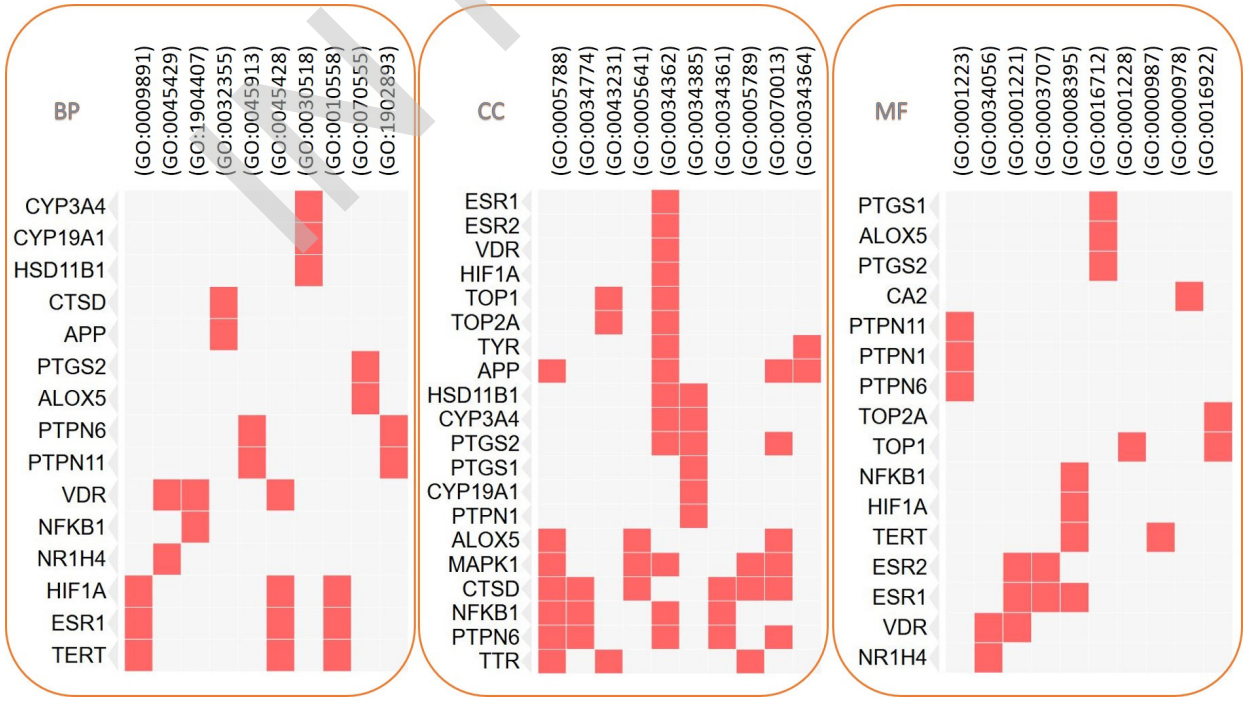


Figure 2: *GO Enrichment Analysis:* Clustergrams displaying the top significantly enriched Gene Ontology terms across Biological Processes, Cellular Components, and Molecular Functions for the 30 common targets. Adjusted p-values are used to rank enrichment significance.

IN PRESS

Table 2: Cytohubba based study of the PPI network identifying hub-genes on the basis of Degree, MCC and Closeness.

Closeness			Degree			MCC		
Rank	Gene	Score	Rank	Gene	Score	Rank	Gene	Score
1	ESR1	22.33	1	ESR1	16	1	ESR1	980
2	NFKB1	22	1	NFKB1	16	2	NFKB1	944
3	PTGS2	21.66	3	PTGS2	15	3	PTGS2	912
4	MAPK1	20.16	4	MAPK1	12	4	HIF1A	901
5	HIF1A	20	4	HIF1A	12	5	MAPK1	898
6	AR	18.66	6	AR	9	6	AR	792
7	CYP3A4	18.25	6	CYP3A4	9	7	ESR2	746
8	ESR2	18.16	8	ESR2	8	8	APP	124
9	CYP19A1	17.75	8	CYP19A1	8	9	PTPN11	54
10	APP	17.33	10	APP	7	10	CYP19A1	53

Table 3: Molecular docking parameters for interactions between the five phytochemicals and targets ***ESR1***, ***NFKB1***, and ***PTGS2***, including binding affinity, total energy, van der Waals, and electrostatic energy.

Sl. No.	Complex	Affinity	Total Energy	vdW Energy	Elec. Energy
1	Ursolic acid-*ESR1*	-8.21	49.83	-8.40	-24.45
2	Loganic acid-*ESR1*	-7.76	10.97	-12.97	-24.94
3	Loganin-ESR1	-7.59	20.44	-13.39	-16.52
4	β-Sitosterol-ESR1	-8.38	40.49	-18.10	-6.73
5	Chlorogenic Acid-*ESR1*	-7.14	5.92	-5.41	-35.89
6	Ursolic acid-*NFKB1*	-7.62	50.80	-9.97	-21.83
7	Loganic acid-*NFKB1*	-6.97	7.98	-1.44	-35.94
8	Loganin-NFKB1	-7.07	14.01	-8.19	-30.78
9	β-Sitosterol-NFKB1	-8.57	38.57	-21.66	-5.72
10	Chlorogenic Acid-*NFKB1*	-6.48	1.97	-3.68	-43.06
11	Ursolic acid-*PTGS2*	-8.31	55.05	-20.07	-7.83
12	Loganic acid-*PTGS2*	-7.67	10.36	-14.39	-21.34
13	Loganin-PTGS2	-7.56	16.56	-16.20	-20.26
14	β-Sitosterol-PTGS2	-8.29	37.73	-20.76	-6.95
15	Chlorogenic Acid-*PTGS2*	-7.53	-2.38	-14.37	-30.06

IN PRESS

–8.305 kcal/mol with *PTGS2*, while β-Sitosterol showed strong binding to *NFKB1* (–8.567 kcal/mol) (Table 3). These findings, representing a convergence of computational predictions and network-based target screening, provide compelling structural evidence for the potential anti-osteoporotic effects of *Dipsacus inermis* through multi-target engagement.

Inhibition of Nitric Oxide

In experiments assessing NO production, the Griess assay revealed a marked, dose-dependent decline in nitrite concentration in the culture supernatants following extract treatment. Untreated, LPS-stimulated macrophages exhibited nitrite levels averaging approximately 20 µM, indicating a significant inflammatory response. In contrast, pre-treatment with the *Dipsacus inermis* extract at 400 µg/mL significantly lowered nitrite accumulation to nearly 9 µM, equating to a reduction of about 55% (Figure 5A). The consistency of this anti-inflammatory effect was confirmed across triplicate assays, and statistical analysis via one-way ANOVA demonstrated significance ($p<0.01$). These findings underscore the potential of the extract to mitigate inflammatory mediator release in activated macrophages.

Inhibition of COX-2 Expression

The evaluation of COX-2 expression by ELISA provided further confirmation on anti-inflammatory properties of the *Dipsacus inermis*. Macrophages stimulated with 1 µg/mL LPS for 24 hr exhibited elevated COX-2 levels, with control samples averaging 625 ± 30 pg/mL. Notably, pre-treatment with the extract resulted

in a substantial downregulation of COX-2 expression, with levels reduced to 315 ± 25 pg/mL (Figure B). Cells were processed using the cell extraction buffer included in the COX-2 kit, and the resultant lysates, clarified by centrifugation at 18,000 × g, yielded reproducible data when assessed at an absorbance of 450 nm. This approximately 50% reduction in COX-2 levels, consistently observed across three independent experiments, demonstrates the extract's efficacy in modulating key inflammatory pathways.

Inhibition of NF-κB

LPS stimulation markedly increased NF-κB p65 levels to 450 pg/mL compared to the unstimulated control (15 pg/mL), confirming macrophage activation. Treatment with *Dipsacus inermis* extract demonstrated a concentration-dependent inhibition of NF-κB activation. At 25, 50, 100, 200, and 400 µg/mL, the extract reduced NF-κB levels to 418.5, 382.5, 328.5, 274.5, and 193.5 pg/mL, respectively, corresponding to 7%, 15%, 27%, 39%, and 57%

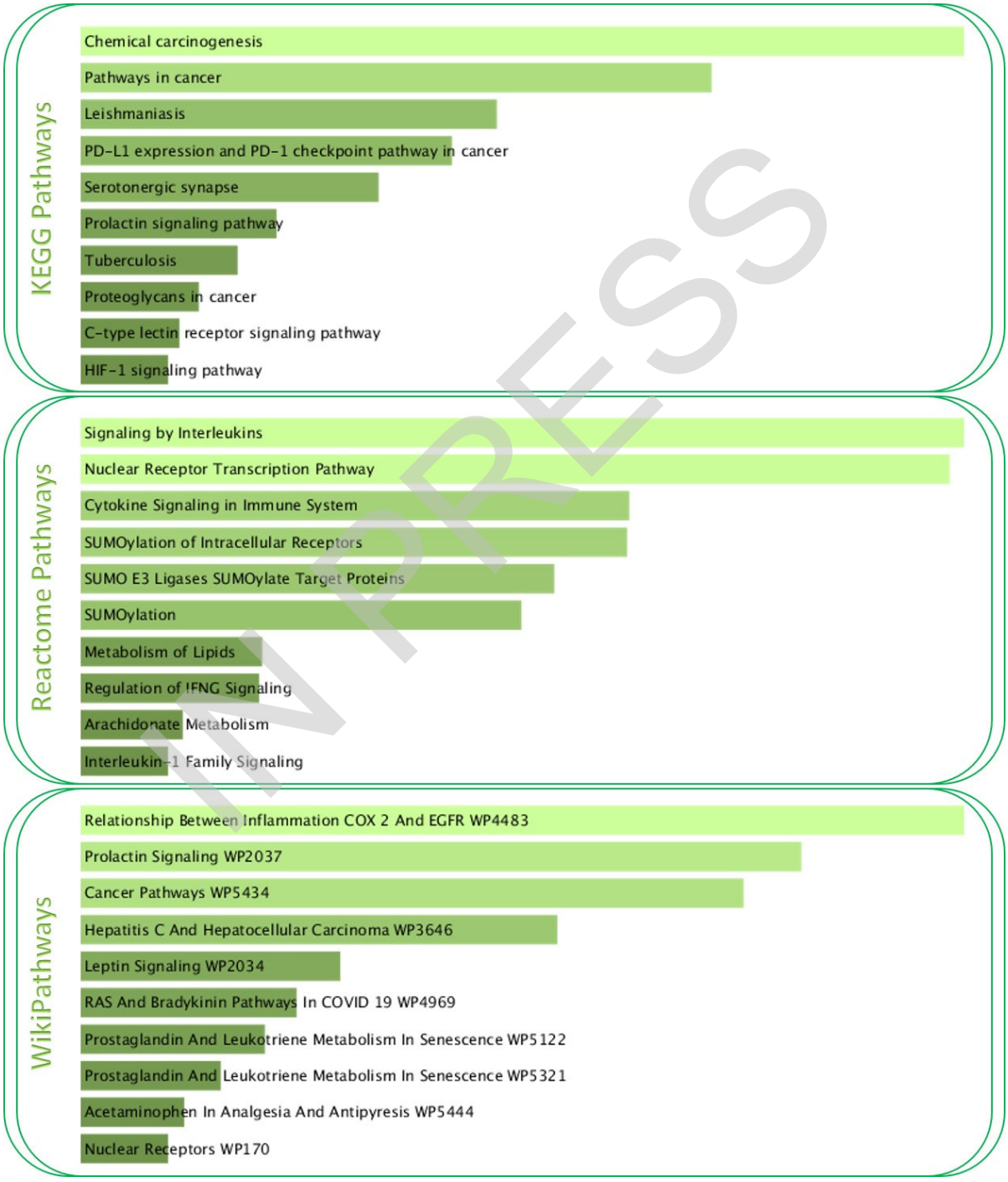


Figure 3: *Pathways Enrichment Analysis:* Graphical representation (such as a dot plot or bar chart) showing significant pathways enriched (from KEGG, Reactome, and WikiPathways) for the 30 common targets. Enrichment is based on adjusted p-values, highlighting key pathways involved in osteoporosis and inflammatory regulation.

IN PRESS

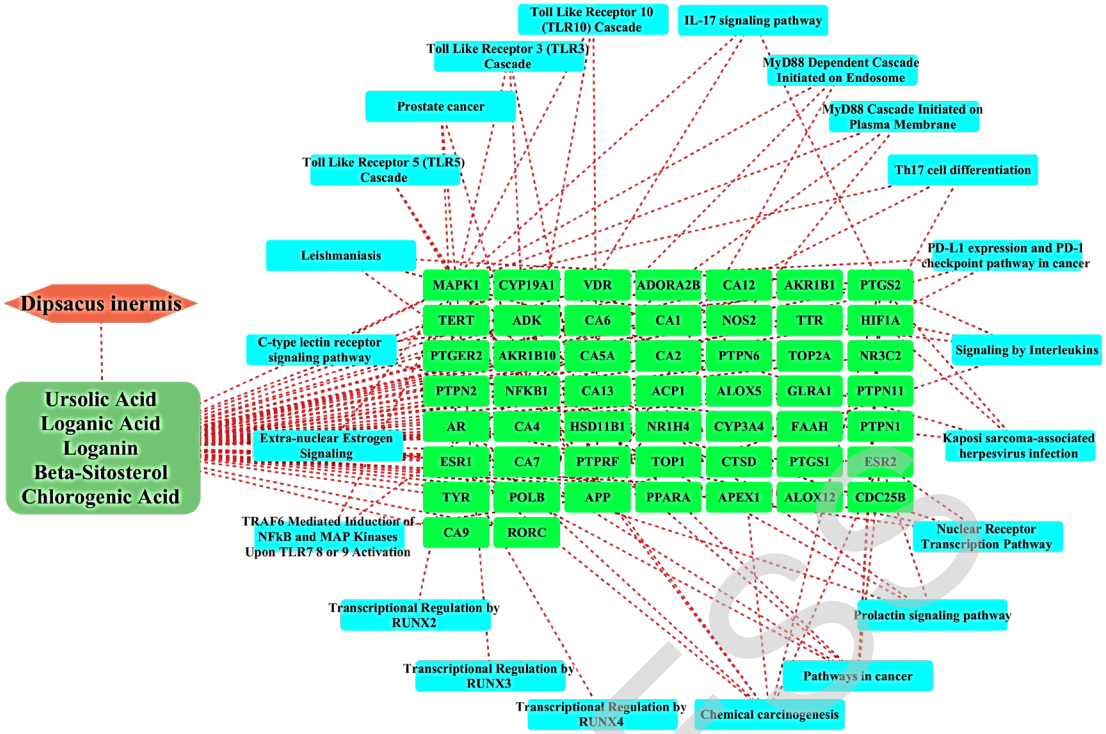


Figure 4: Network visualization of plant-compounds-targets-pathways interactions enriched from KEGG, Reactome, and WikiPathways. The network highlights the common targets modulated by compounds from Dipsacus inermis, illustrating its multi-target therapeutic potential in osteoporosis. All pathway enrichments were based on adjusted p-values, ensuring statistical robustness and biological relevance.

inhibition relative to LPS-treated cells (Figure C and 5D). These results indicate that *Dipsacus inermis* exerts a dose-dependent anti-inflammatory effect in J774A.1 macrophages by suppressing LPS-induced NF-κB activation.

Cytotoxicity against J774A.1 Cells

Cytotoxic evaluation of the *Dipsacus inermis* extract using the MTT assay revealed a concentration-dependent impact on the viability of J774A.1 macrophages. At lower extract concentrations (25 and 50 µg/mL), proliferation stayed remarkably high (>90%), indicating minimal cytotoxic interference under these conditions. Nevertheless, a significant decrease in proliferation was seen with increasing dosage; treatment with 400 µg/mL resulted in a viability reduction to 65%, while the highest concentration tested (800 µg/mL) further diminished cell viability to approximately 45% relative to untreated controls (Figure 6). These statistically significant ($p<0.05$) results, suggest that while the extract exhibits potent anti-inflammatory effects at specific concentrations, higher doses may exert cytotoxic effects on macrophage viability. The assay outcomes were verified across multiple replicates, ensuring consistency and reliability of the observed cytotoxic profiles.

DISCUSSION

The integrated application of network pharmacology, molecular docking, and experimental assays in our study has provided compelling evidence for the anti-osteoporotic potential of *Dipsacus inermis* through the modulation of key molecular targets-namely *ESR1, NFKB1*, and *PTGS2*/COX-2-which are also relevant to other inflammatory conditions. The convergence of our data from target prediction, molecular docking, and *in vitro* inflammatory assays underscores a multi-target mechanism that could translate into novel therapeutic strategies for osteoporosis and additional pathologies characterized by dysregulated estrogen signalling and chronic inflammation.

Our network pharmacology analysis initially identified many targets associated with both the plant-derived phytochemicals and osteoporosis. The intersection of these data resulted in 30 common targets, among which *ESR1, NFKB1*, and *PTGS2*/COX-2 emerged as key nodes based on PPI network topology and hub gene analysis. Molecular docking studies further substantiated these findings, demonstrating that phytochemicals such as Ursolic acid, Loganic acid, and β-Sitosterol bind effectively to these targets with favorable binding energies. For instance, Ursolic acid exhibited binding affinities of –8.214 with *ESR1* and –8.305 with *PTGS2*, while β-Sitosterol showed an affinity of –8.567 with *NFKB1*. These *in silico* observations provide a structural and

IN PRESS

thermodynamic basis for the biological activity observed in our experimental assays.

ESR1, or Estrogen Receptor 1, is important in bone metabolism by arbitrating the protective effects of estrogen on bone density and quality.[23] Its activation is well-known for promoting osteoblastic activity and inhibiting osteoclastic bone resorption-a mechanism that is particularly relevant in postmenopausal osteoporosis.[24] Our docking results indicate that the bioactive compounds in *Dipsacus inermis* can favorably interact with *ESR1*, suggesting that these phytochemicals might enhance estrogenic signalling in bone tissue. Recent studies by Zhivodernikov *et al.*, 2023 and Chen *et al.*, 2024 have reported that enhancing *ESR1* activity can mitigate bone loss and improve skeletal strength in osteoporotic models.[24,25] In this context, our findings resonate well with these contemporary studies, further supporting the therapeutic potential of targeting *ESR1* not only in osteoporosis but also in estrogen-related disorders such as certain breast and reproductive cancers.

NFKB1 is a crucial transcription factor involved in the control of responses to inflammation.[26] It leads to the transcription of numerous pro-inflammatory cytokines and chemokines that contribute to chronic inflammation-a hallmark of not only osteoporosis but also conditions such as rheumatoid arthritis and atherosclerosis.[27] The observed reduction in nitrite production in our LPS-stimulated macrophage assays supports the impression that *Dipsacus inermis* extract can modulate *NFKB1* activity, thereby diminishing inflammatory mediator release. This inhibitory effect on *NFKB1* aligns with recent report by Múnera-Rodríguez *et al.*, 2024 that have highlighted the role of NF-κB inhibition for reducing inflammation and tissue degradation in autoimmune and chronic inflammatory diseases.[28] Our molecular docking data, which indicate significant binding interactions between the phytochemicals and *NFKB1*, and also *in vitro* validation showing inhibition of NFKB, further validate the extract's potential to directly interfere with this pro-inflammatory pathway.

IN PRESS

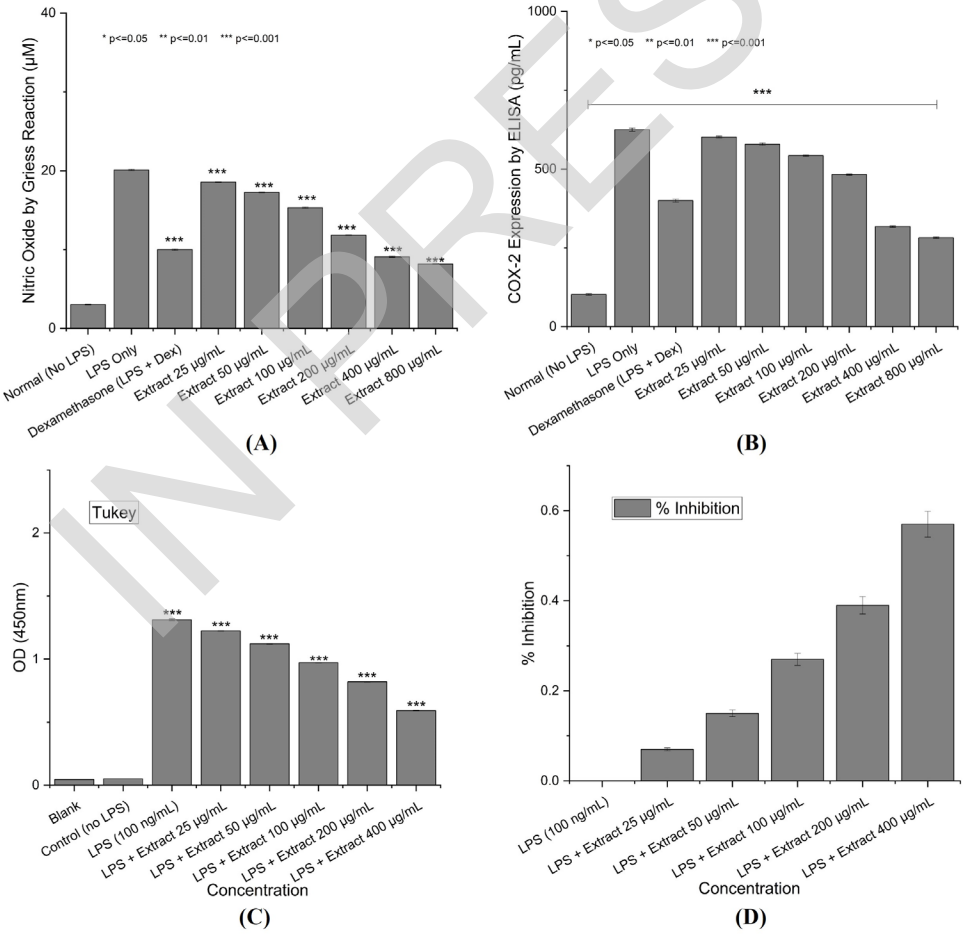


Figure 5: (A) Inhibition of Nitric Oxide Production: Graph depicting the dose-dependent reduction in nitrite concentration, measured by the Griess assay, in LPS-stimulated macrophages following treatment with varying concentrations of Dipsacus inermis extract. (B) Reduction in COX-2 Expression: Bar graph showing the significant decrease in COX-2 levels (pg/mL) in macrophages pre-treated with the extract compared to the LPS-stimulated control, as determined by ELISA. (C) Effect of Dipsacus inermis extract on NF-κB p65 activation in LPS-stimulated J774A.1 macrophages. OD_{450} readings were recorded from ELISA to determine NF-κB levels. The extract exhibited dose-dependent inhibition of NF-κB activation, with a gradual reduction in OD values at increasing concentrations (25–400 µg/mL). (D) Percent inhibition of NF-κB p65 activation in J774A.1 macrophages upon extract treatment, plotted against concentration. Data confirm dose-dependent suppression of LPS-induced inflammatory signaling.

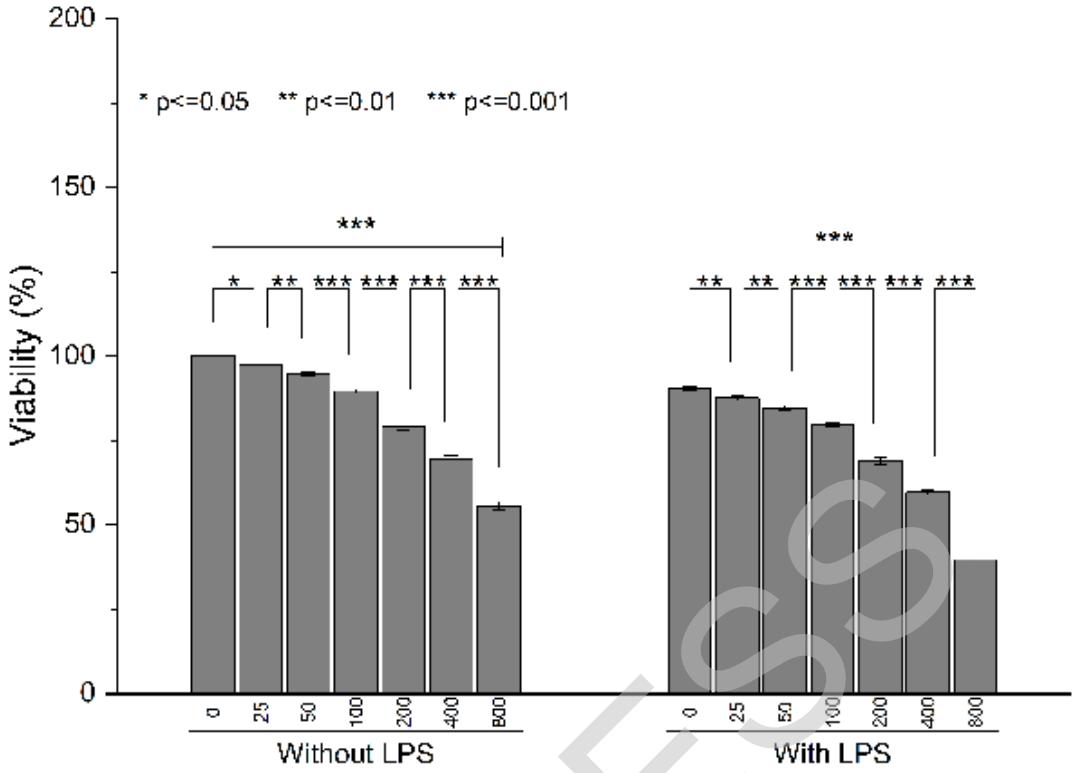


Figure 6: Cytotoxicity Assessment via MTT Assay: Bar graph summarizing cell viability (%) of J774A.1 macrophages treated with increasing concentrations (0, 25, 50, 100, 200, 400, and 800 µg/mL) of Dipsacus inermis extract, demonstrating a dose-dependent decrease in cell viability.

PTGS2, known as COX-2, is an enzyme critical in the biosynthesis of prostaglandins, which are key mediators of inflammation.[29] Elevated COX-2 levels are associated with increased inflammatory responses and pain in a variety of conditions, including osteoarthritis, rheumatoid arthritis, and certain cancers.[30] Our *in vitro* experiments demonstrated a significant reduction in COX-2 expression upon treatment with the *Dipsacus inermis* extract, with a nearly 50% decrease in protein levels compared to LPS-stimulated controls. This reduction was mirrored by our docking studies, where phytochemicals exhibited considerable binding affinity to *PTGS2*, with binding energies suggesting effective inhibition. Contemporary studies by Chun *et al.* 2024 and Wu *et al.*, 2022 have reported that targeting COX-2 not only ameliorates inflammatory pain but also modulates tumorigenesis in inflammation-associated cancers.[31,32] The ability of *Dipsacus inermis*-derived compounds to interact with COX-2, therefore, suggests potential applications in a broader spectrum of inflammatory and neoplastic conditions.

Our study presents a comprehensive approach for determination of the molecular mechanisms underlying the anti-osteoporotic effects of *Dipsacus inermis*. The identification of *ESR1, NFKB1*, and *PTGS2* as central targets, along with the demonstration of significant binding interactions and functional inhibition in cell-based assays, provides strong evidence for the therapeutic relevance of this medicinal plant. When compared with recent literature published post-2020, our findings not only corroborate the emerging role of these targets in osteoporosis but also highlight their potential involvement in other pathologies, including various inflammatory and hormone-related disorders. This multi-target, multi-pathway interaction model opens promising avenues that leverage the inherent polypharmacology of traditional medicinal plants like *Dipsacus inermis*.

CONCLUSION

This study reveals that *Dipsacus inermis* possesses strong anti-osteoporotic potential through a multi-target mechanism involving *ESR1, NFKB1*, and *PTGS2/COX-2*. Phytochemical screening identified several compounds, refined to five key bioactives based on strict criteria. Network pharmacology and PPI analyses highlighted overlapping osteoporosis-related targets and hub genes linked to bone metabolism and inflammation. *In vitro* assays showed dose-dependent inhibition of nitric oxide and *COX-2* expression with acceptable cell viability at lower doses. Molecular docking confirmed stable binding of the phytochemicals to *ESR1, NFKB1,* and *PTGS2*. Overall, these results support *Dipsacus inermis* as a promising multi-target candidate for osteoporosis and related inflammatory disorders warranting further clinical investigations.

IN PRESS

ACKNOWLEDGEMENT

None.

ABBREVIATIONS

TCMID: Traditional Chinese Medicine Integrated Database; **MW:** Molecular Weight; **Da:** Dalton; **HBA:** Hydrogen Bond Acceptor; **HBD:** Hydrogen Bond Donor; **PSA:** Polar Surface Area; **PPI:** Protein–Protein Interaction; **GO:** Gene Ontology; BP: Biological Process; **CC:** Cellular Component; **MF:** Molecular Function; **KEGG:** Kyoto Encyclopedia of Genes and Genomes; **DMEM:** Dulbecco's Modified Eagle Medium; **FBS:** Fetal Bovine Serum; **DMSO:** Dimethyl Sulfoxide; **ELISA:** Enzyme-Linked Immunosorbent Assay; **LPS:** Lipopolysaccharide; **NO:** Nitric Oxide; **MTT:** 3-(4,5-Dimethylthiazol-2-yl)-2,5-diphenyltetrazolium Bromide; **GIFTS:** Gene Inference and Functionality Scoring Tool.

CONFLICT OF INTEREST

The authors declare that there is no conflict of interest.

FUNDING

This research was conducted without any external funding support.

SUMMARY

The study began by mining the Traditional Chinese Medicine Integrated Database (TCMID) for phytochemicals in *Dipsacus inermis*, identifying 15 candidates. Applying drug-likeness filters (molecular weight 200–500 Da, Lipinski's rule), five compounds were selected-ursolic acid, loganic acid, loganin, β-sitosterol, and chlorogenic acid-ensuring optimal physicochemical properties for further analysis. Targets of these five compounds were predicted via SuperPred (110 targets), SwissTargetPrediction (116), and TCMID (65). Intersection of at least two sources yielded 51 high-confidence targets. Separately, GeneCards returned 7,231 osteoporosis-related targets, which, after filtering for GIFTS scores ≥ 60%, narrowed to 1,038 disease-specific targets. Comparison between phytochemical and disease lists revealed 30 overlapping proteins, suggesting potential mechanisms for anti-osteoporotic activity. A Protein–Protein Interaction (PPI) network built in STRING (30 nodes, 89 edges; $p = 1.11 \times 10^{16}$) and visualized in Cytoscape highlighted network topology (average degree = 5.93, clustering coefficient = 0.526). Cytohubba identified ten hub genes-*ESR1, NFKB1, PTGS2*, MAPK1, HIF1A, AR, CYP3A4, ESR2, CYP19A1, and APP-central to bone metabolism and inflammatory regulation. Enrichment analyses with Enrichr underscored significant Gene Ontology terms (e.g., nitric oxide biosynthesis, steroid hormone signaling) and pathways across KEGG, Reactome, and WikiPathways, reinforcing a multi-target mode of action. Molecular docking against *ESR1, NFKB1*, and *PTGS2* showed strong binding affinities (e.g., β-sitosterol–*NFKB1*: –8.567 kcal/mol), corroborating the network predictions. *In vitro* assays demonstrated dose-dependent inhibition of nitric oxide production (up to 55% reduction), COX-2 expression (~50% reduction), and NF-κB activation (up to 57% inhibition) in LPS-stimulated macrophages, with significant cytotoxicity at higher doses against J774A.1 macrophages.

REFERENCES

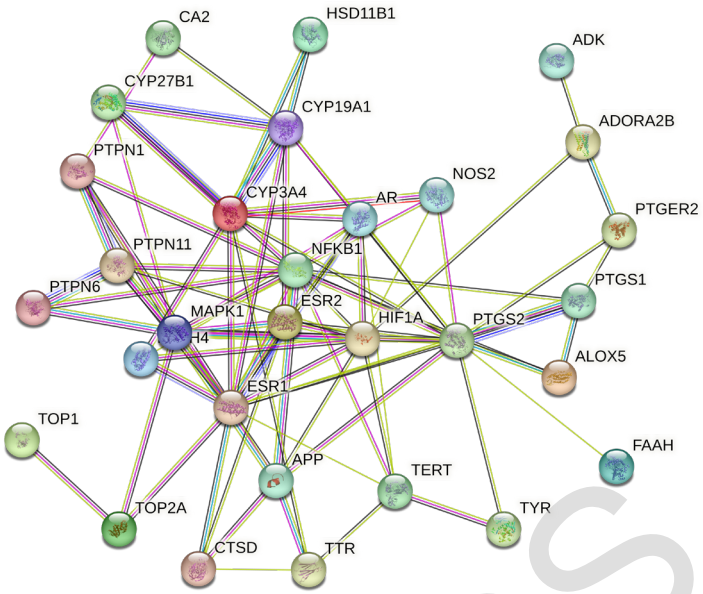
1. Chadha M, Chaddha R, Divakar H, Kalyan H, Seth S, Shah P. Osteoporosis: epidemiology, pathogenesis, evaluation and treatment. Open Journal of Orthopedics. 2022;12(4):153-82.
2. Aibar-Almazán A, Voltes-Martínez A, Castellote-Caballero Y, Afanador-Restrepo DF, Carcelén-Fraile MD, López-Ruiz E. Current status of the diagnosis and management of osteoporosis. International journal of molecular sciences. 2022;23(16):9465.
3. Liang B, Burley G, Lin S, Shi YC. Osteoporosis pathogenesis and treatment: existing and emerging avenues. Cellular and Molecular Biology Letters. 2022;27(1):72.
4. Adami G, Fassio A, Gatti D, Viapiana O, Benini C, Danila MI, Saag KG, Rossini M. Osteoporosis in 10 years time: a glimpse into the future of osteoporosis. Therapeutic Advances in Musculoskeletal Disease. 2022;14:1759720X221083541.
5. Xin WA, Zi-Yi WA, Shao LI. TCM network pharmacology: a new trend towards combining computational, experimental and clinical approaches. Chinese journal of natural medicines. 2021;19(1):1-1.
6. Jiashuo WU, ZHANG F, Zhuangzhuang LI, Weiyi JI, Yue SH. Integration strategy of network pharmacology in Traditional Chinese Medicine: a narrative review. Journal of Traditional Chinese Medicine. 2022;42(3):479.
7. Muhammed MT, Aki-Yalcin E. Molecular docking: Principles, advances, and its applications in drug discovery. Letters in Drug Design and Discovery. 2024;21(3):480-95.
8. Wani I, Manzoor N, Singh KP, Pal A. Evaluation of antioxidant property of hydro-alcohol root extract from *Thymus linearis* benth. And *Dipsacus inermis* Wall. In kashmir valley. Global Journal of Research on Medicinal Plants and Indigenous Medicine. 2017;6(11):121-6.
9. Hassan S, Sajjad N, Khan SU, Gupta S, Bhat MA, Ali R, Ahmad Z, Ganie SA, Hamid R. *Dipsacus inermis* Wall. modulates inflammation by inhibiting NF-κB pathway: an *in vitro* and *in vivo* study. Journal of Ethnopharmacology. 2020;254:112710.
10. Tao Y, Chen L, Yan J. Traditional uses, processing methods, phytochemistry, pharmacology and quality control of *Dipsacus asper* Wall. ex CB Clarke: a review. Journal of Ethnopharmacology. 2020;258:112912.
11. Huang L, Xie D, Yu Y, Liu H, Shi Y, Shi T, Wen C. TCMID 2.0: a comprehensive resource for TCM. Nucleic acids research. 2018; 46(D1):D1117-20.
12. Marufatuzzahan M, Mondal S, Robin TB, Raihan M, Toureen A, Alam MT, Afrin D. Molecular Dynamics Simulations and Reverse Docking Approaches for Identification of Novel Drug Candidates Against Aeromonas hydrophila. Chinese Journal of Analytical Chemistry. 2025: 100616.
13. Daina A, Michielin O, Zoete V. SwissTargetPrediction: updated data and new features for efficient prediction of protein targets of small molecules. Nucleic acids research. 2019; 47(W1):W357-64.
14. Gallo K, Goede A, Preissner R, Gohlke BO. SuperPred 3.0: drug classification and target prediction-a machine learning approach. Nucleic acids research. 2022; 50(W1):W726-31.
15. Stelzer G, Rosen N, Plaschkes I, Zimmerman S, Twik M, Fishilevich S, Stein TI, Nudel R, Lieder I, Mazor Y, Kaplan S. The GeneCards suite: from gene data mining to disease genome sequence analyses. Current protocols in bioinformatics. 2016;54(1):1-30.
16. Li Z, Ji L, Dai X, Xiao Y. Integrated Computational Chemistry and Experimental Analysis of Fructus Ligustri to Target Chemoresistant Ovarian Cancer Cells. Iranian Journal of Chemistry and Chemical Engineering. 2025;44(9):2308-23.
17. Szklarczyk D, Kirsch R, Koutrouli M, Nastou K, Mehryary F, Hachilif R, Gable AL, Fang T, Doncheva NT, Pyysalo S, Bork P. The STRING database in 2023: protein–protein association networks and functional enrichment analyses for any sequenced genome of interest. Nucleic acids research. 2023; 51(D1):D638-46.
18. Guedes IA, da Silva MM, Galheigo M, Krempser E, de Magalhães CS, Barbosa HJ, Dardenne LE. DockThor-VS: a free platform for receptor-ligand virtual screening. Journal of Molecular Biology. 2024;436(17):168548.
19. Hosfield DJ, Weber S, Li NS, Sauvage M, Joiner CF, Hancock GR, Sullivan EA, Ndukwe E, Han R, Cush S, Lainé M. Stereospecific lasofoxifene derivatives reveal the interplay between estrogen receptor alpha stability and antagonistic activity in ESR1 mutant breast cancer cells. Elife. 2022;11:e72512.
20. Kurumbail RG, Stevens AM, Gierse JK, McDonald JJ, Stegeman RA, Pak JY, Gildehaus D, Iyashiro JM, Penning TD, Seibert K, Isakson PC. Structural basis for selective inhibition of cyclooxygenase-2 by anti-inflammatory agents. Nature. 1996;384(6610):644-8.
21. Ghosh G, Duyne GV, Ghosh S, Sigler PB. Structure of NF-κB p50 homodimer bound to a κB site. Nature. 1995;373(6512):303-10.

IN PRESS

22. Xie Z, Bailey A, Kuleshov MV, Clarke DJ, Evangelista JE, Jenkins SL, Lachmann A, Wojciechowicz ML, Kropiwnicki E, Jagodnik KM, Jeon M. Gene set knowledge discovery with Enrichr. Current protocols. 202;1(3):e90.
23. Holliday KL, Pye SR, Thomson W, Boonen S, Borghs H, Vanderschueren D, Gielen E, Huhtaniemi IT, Adams JE, Ward KA, Bartfai G. The *ESR1* (6q25) locus is associated with calcaneal ultrasound parameters and radial volumetric bone mineral density in European men. PLoS One. 2011;6(7):e22037.
24. Zhivodernikov IV, Kirichenko TV, Markina YV, Postnov AY, Markin AM. Molecular and cellular mechanisms of osteoporosis. International journal of molecular sciences. 2023;24(21):15772.
25. Chen J, Hao Z, Li H, Wang J, Chen T, Wang Y, Shi G, Wang J, Wang Z, Zhang Z, Li J. Osteoporotic osseointegration: therapeutic hallmarks and engineering strategies. Theranostics. 2024;14(10):3859.
26. Moneva-Sakelarieva M, Kobakova Y, Konstantinov S, Momekov G, Ivanova S, Atanasova V, Chaneva M, Tododrov R, Bashev N, Atanasov P. The role of the transcription factor NF-kB in the pathogenesis of inflammation and carcinogenesis. Modulation capabilities. Pharmacia. 2025;72:1-3.
27. Barnabei L, Laplantine E, Mbongo W, Rieux-Laucat F, Weil R. NF-κB: at the borders of autoimmunity and inflammation. Frontiers in Immunology. 2021;12:716469.
28. Múnera-Rodríguez AM, Leiva-Castro C, Sobrino F, López-Enríquez S, Palomares F. Sulforaphane-mediated immune regulation through inhibition of NF-kB and MAPK signaling pathways in human dendritic cells. Biomedicine and Pharmacotherapy. 2024;177:117056.
29. Saleem M, Iftikhar A, Asif M, Hussain K, Alamgeer, Shah PA, Saleem A, Akhtar MF, Tanzeem M, Yaseen HS. Asphodelus tenuifolius extracts arrested inflammation and arthritis through modulation of TNF-α, NF-κB, ILs, and COX-2 activities in *in vivo* models. Inflammopharmacology. 2021;29:483-97.
30. Paul S, Modak D, Chattaraj S, Nandi D, Sarkar A, Roy J, Chaudhuri TK, Bhattacharjee S. Aloe vera gel homogenate shows anti-inflammatory activity through lysosomal membrane stabilization and downregulation of TNF-α and Cox-2 gene expressions in inflammatory arthritic animals. Future Journal of Pharmaceutical Sciences. 2021;7:1-8.
31. Chun KS, Kim EH, Kim DH, Song NY, Kim W, Na HK, Surh YJ. Targeting cyclooxygenase-2 for chemoprevention of inflammation-associated intestinal carcinogenesis: An update. Biochemical Pharmacology. 2024: 116259.
32. Wu B, Sodji QH, Oyelere AK. Inflammation, fibrosis and cancer: mechanisms, therapeutic options and challenges. Cancers. 2022;14(3):552.

Cite this article: Min T, Li S, Zhang X. Multi-Target Mechanisms of Dipsacus inermis Against Osteoporosis via Inhibition of Nitric Oxide and NF-κB/COX-2 Pathway. Indian J of Pharmaceutical Education and Research. 2027;61(1):10.5530/ijper.20262572.

IN PRESS



Suppl. Figure S1: PPI network from String database.

Suppl. Table S1: ***Intersection of Predicted Targets Across Databases:*** **This supplementary table lists the 51 targets common to at least two of the three databases (SuperPred, SwissTargetPrediction, and TCMID) used for target prediction of the selected phytochemicals and the plant.**

Sl. No.	Type	Gene Name
1	Common All	CDC25B
2	Common All	PTGS1
3	Common All	PTPN1
4	Common All	PTPN11
5	Common All	PTPN2
6	Common All	AKR1B10
7	Sup-Swis	ADK
8	Sup-Swis	ADORA2B
9	Sup-Swis	ALOX12
10	Sup-Swis	AR
11	Sup-Swis	ESR2
12	Sup-Swis	FAAH
13	Sup-Swis	GLRA1
14	Sup-Swis	NR3C2
15	Sup-Swis	PTGER2
16	Sup-Swis	TERT
17	Sup-Swis	VDR
18	Sup-TMID	APEX1
19	Sup-TMID	CTSD
20	Sup-TMID	CYP3A4
21	Sup-TMID	HIF1A
22	Sup-TMID	MAPK1
23	Sup-TMID	NFKB1
24	Sup-TMID	TOP2A
25	Sup-TMID	TTR
26	Sup-TMID	AKR1B1
27	TMID-Swiss	RORC
28	TMID-Swiss	POLB
29	TMID-Swiss	PTPRF
30	TMID-Swiss	HSD11B1
31	TMID-Swiss	ACP1
32	TMID-Swiss	PTPN6
33	TMID-Swiss	NOS2
34	TMID-Swiss	PTGS2
35	TMID-Swiss	CYP19A1
36	TMID-Swiss	PPARA
37	TMID-Swiss	TOP1
38	TMID-Swiss	NR1H4
39	TMID-Swiss	ALOX5
40	TMID-Swiss	ESR1
41	TMID-Swiss	CA2
42	TMID-Swiss	CA1
43	TMID-Swiss	CA12
44	TMID-Swiss	CA9
45	TMID-Swiss	TYR
46	TMID-Swiss	CA7
47	TMID-Swiss	CA4
48	TMID-Swiss	CA13
49	TMID-Swiss	CA5A
50	TMID-Swiss	CA6
51	TMID-Swiss	APP

IN PRESS

Suppl. Table S2: ***Osteoporosis-Associated Targets Identified from GeneCards.*** **This supplementary table details the 1038 osteoporosis-related targets, refined from an initial list of 7231 targets using a GIFTS score threshold of ≥60%.**

Suppl. Table S3: ***Gene-ontology analysis.*** **Gene ontologies shown for network identified hub genes using Enrichr data base.**

Name	Term	Genes
BP		
Positive Regulation of Biosynthetic Process	(GO:0009891)	APP;PTGS2;ESR1;HIF1A
Positive Regulation of Nitric Oxide Biosynthetic Process	(GO:0045429)	APP;PTGS2;ESR1
Positive Regulation of Nitric Oxide Metabolic Process	(GO:1904407)	APP;PTGS2;ESR1
Response to Estradiol	(GO:0032355)	ESR1;CYP19A1;ESR2
Positive Regulation of Carbohydrate Metabolic Process	(GO:0045913)	APP;HIF1A;NFKB1
Regulation of Nitric Oxide Biosynthetic Process	(GO:0045428)	APP;PTGS2;ESR1
Nuclear Receptor-Mediated Steroid Hormone Signaling Pathway	(GO:0030518)	MAPK1;ESR1;ESR2
Negative Regulation of Macromolecule Biosynthetic Process	(GO:0010558)	APP;ESR1;HIF1A;NFKB1
Response to Interleukin-1	(GO:0070555)	APP;HIF1A;NFKB1
Regulation of miRNA Transcription	(GO:1902893)	APP;ESR1;HIF1A
CC		
Endoplasmic Reticulum Lumen	(GO:0005788)	APP;MAPK1;PTGS2
Secretory Granule Lumen	(GO:0034774)	APP;MAPK1;NFKB1
Intracellular Membrane-Bounded Organelle	(GO:0043231)	APP;MAPK1;PTGS2;CYP3A4;ESR1;HIF1A;NFKB1;ESR2
Nuclear Envelope Lumen	(GO:0005641)	APP
Low-Density Lipoprotein Particle	(GO:0034362)	APP
Triglyceride-Rich Plasma Lipoprotein Particle	(GO:0034385)	APP
Very-Low-Density Lipoprotein Particle	(GO:0034361)	APP
Endoplasmic Reticulum Membrane	(GO:0005789)	PTGS2;CYP3A4;CYP19A1
Intracellular Organelle Lumen	(GO:0070013)	APP;MAPK1;PTGS2
High-Density Lipoprotein Particle	(GO:0034364)	APP
MF		
Transcription Coactivator Binding	(GO:0001223)	ESR1;HIF1A;NFKB1
Estrogen Response Element Binding	(GO:0034056)	ESR1;ESR2
Transcription Coregulator Binding	(GO:0001221)	ESR1;HIF1A;NFKB1
Nuclear Steroid Receptor Activity	(GO:0003707)	ESR1;ESR2
Steroid Hydroxylase Activity	(GO:0008395)	CYP3A4;CYP19A1
Oxidoreductase, Paired Donors, W Incorp or Reduc of O2, Reduced Flavin or Flavoprotein as One Donor, and Incorp of O	(GO:0016712)	CYP3A4;CYP19A1
DNA-binding Transcription Activator Activity, RNA Polymerase II-specific	(GO:0001228)	ESR1;HIF1A;NFKB1
Cis-Regulatory Region Sequence-Specific DNA Binding	(GO:0000987)	ESR1;HIF1A;NFKB1;ESR2
RNA Polymerase II Cis-Regulatory Region Sequence-Specific DNA Binding	(GO:0000978)	ESR1;HIF1A;NFKB1;ESR2
Nuclear Receptor Binding	(GO:0016922)	ESR1;HIF1A

IN PRESS